IJRCS

International Journal of Robotics and Control Systems
Vol. 6, No. 2, 2026, pp. 1233-1250
ISSN 2775-2658
http://pubs2.ascee.org/index.php/ijrcs

ASCEE

Sliding Mode Extremum Seeking Control Based PID of a Quadrotor

Ouassila Bourebia [a,1,*], Ilyes Boulkaibet [b,2], Nadhira Khezami [b,3]

[a] Automatics and Robotic Laboratory, Faculty of Sciences and Technology, Electronics Department, Constantine 1 University, Constantine, Algeria
[b] College of Engineering and Technology, American University of the Middle East, Kuwait
[1] bourebia.ouassila@umc.edu.dz; [2] ilyes.boulkaibet@aum.edu.kw; [3] Nadhira.khezami@aum.edu.kw
* Corresponding Author

ARTICLE INFO

Article history
Received January 19, 2026
Revised March 05, 2026
Accepted April 21, 2026

Keywords
Sliding Mode Control;
Extremum Seeking Control;
PID Controller;
Quadrotor;
Nonlinear Control

ABSTRACT

This paper presents a modern methodology for controlling a quadrotor system through the automatic tuning of Proportional-Integral-Derivative (PID) controller, using the Sliding Mode Extremum Seeking Control (SMESC) framework. The proposed approach combines the inherent robustness of Sliding Mode Control (SMC) with the adaptive, model-free optimization capability of Extremum Seeking Control (ESC), enabling online performance optimization without requiring an accurate system model. In contrast to offline tuning methods, the proposed SMESC-based PID tuning continuously adjusts the control gains during operation, based solely on real-time tracking error information, ensuring robustness against disturbances and parameter variations. as well as time-varying operating conditions, and enabling real-time adjustment of PID gains. Quantitatively, the proposed SMESC approach improves the rise time by approximately 40% as well as the settling time by about 30% compared to the PSO-based PID controller. In addition, the proposed approach significantly reduces overshoot by more than 60%. The findings demonstrate that the SMESC-PID controller delivers markedly enhanced stability and overall performance when compared with the conventional PSO-PID-based approach. To further evaluate robustness, the system was subjected to additive external disturbances in order to assess the stability and resilience of the proposed controller under challenging operating conditions. The simulation results clearly show that the proposed control methodology significantly outperforms traditional tuning techniques, providing superior disturbance-rejection capabilities and substantially improved stability in quadrotor flight control.

1. Introduction

Controlling a quadrotor constitutes a challenging engineering problem owing to its intrinsically unstable and highly nonlinear dynamics [1], [2]. Although the system exhibits six degrees of freedom, it is actuated by only four independent control inputs [3]-[5], thereby resulting in an underactuated configuration that necessitates the implementation of advanced and sophisticated control strategies [6], [7], Achieving accurate trajectory tracking and stable flight control requires effectively addressing the dynamics of a quadrotor are inherently complex due to the significant interaction between its

translational and rotational motions [8]. Movements along the linear axes (x, y, z) are strongly influenced by the rotations around roll, pitch, and yaw, meaning that a change in orientation directly affects the vehicle's position in space. This coupling makes precise control challenging, as controllers must simultaneously account for both angular and linear respons [9], [10] while simultaneously accounting for external disturbances and parametric uncertainties. Consequently, the development of robust and adaptive control methodologies has become a prominent and central research theme within the domain of unmanned aerial vehicle (UAV) systems [11], [12].

The Proportional–Integral–Derivative (PID) controller is widely adopted in quadrotor control applications due to its inherent simplicity [13], straightforward implementation, and intuitive tuning procedure. Nevertheless, classical PID control strategies [14] often exhibit limited performance when confronted with the strong nonlinearities and rapidly varying dynamics characteristic of quadrotor systems [15], [16]. Demonstrated that reformulating the derivative action to operate on the plant state rather than on the tracking error leads to notable improvements in robustness and closed-loop stability [17]. This modification also contributes to the reduction of excessive control efforts induced by abrupt variations in reference signals. Despite these advantages, the reliance on manual tuning of PID parameters remains a critical limitation, as it is highly dependent on the expertise of control engineers and is frequently constrained by the limited availability of accurate system models.

To overcome these limitations, a wide range of approaches have been proposed to automate PID parameter tuning with meta-heuristic optimization techniques [18], [12]-such as Particle Swarm Optimization (PSO) [19], [20], Genetic Algorithms (GA) [21], and the Crow Search Algorithm (CSA) [22]-receiving increasing attention. These methods typically optimize controller parameters in an offline framework by minimizing predefined performance indices [23], including tracking error or energy consumption [24]-[26]. Although effective under static operating conditions, their offline nature inherently restricts their ability to adapt to real-time disturbances or continuously evolving system dynamics [27].

To address these limitations, adaptive, model-free strategies have been developed. Extremum Seeking Control (ESC), as applied in [28]-[30], constitutes a promising online optimization methodology that iteratively adjusts PID parameters by minimizing a cost function derived from tracking performance metrics. ESC operates without necessitating an explicit system model, rendering it particularly suitable for applications characterized by complex or uncertain dynamics. By introducing small perturbations and analyzing the resultant system response, ESC converges in real time to near-optimal controller parameters [31]. Its application to quadrotor PID tuning has demonstrated superior transient performance and enhanced disturbance rejection when compared to both classical PID schemes and metaheuristically tuned controllers [32]. Concurrently, Sliding Mode Control (SMC) has gained widespread adoption owing to its inherent robustness against matched disturbances and its finite-time convergence properties. In quadrotor systems, SMC has demonstrated effectiveness in maintaining reliable performance under uncertain conditions, although it may exhibit chattering due to the discontinuous nature of its control law [33], [34]. To mitigate this phenomenon, higher-order and adaptive sliding mode techniques have been proposed [35], [36], while hybrid frameworks have combined SMC with fuzzy logic, neural networks, or fractional-order elements to further enhance system performance [37]-[39].

Building upon these advancements, contemporary research has increasingly focused on merging optimization algorithms with robust control methodologies to enhance adaptability [40], resilience, and real-time performance. In particular, the unification of Extremum Seeking Control (ESC) and Sliding Mode Control (SMC) [41], collectively referred to as Sliding Mode Extremum Seeking Control (SMESC), has demonstrated remarkable success in domains such as wind energy conversion [42] and precision motion systems [43], consistently delivering superior tracking capabilities and heightened robustness under fluctuating operating conditions [44]-[47]. In particular, the combination of extremum seeking control with sliding mode control has been shown to significantly improve both stability and performance, as reported in [48]. Crucially, this hybrid framework preserves the inherent disturbance-rejection properties of SMC while effectively mitigating the chattering phenomenon and accelerating convergence when compared to standalone ESC [49], [50].

Despite these promising outcomes, the deployment of SMESC in the context of quadrotor PID tuning remains conspicuously absent from the existing literature. To the best of our knowledge, no prior work has attempted to adapt and implement this hybrid methodology for quadrotor systems. In this regard, the present study introduces a pioneering contribution by applying SMESC to quadrotor control, thereby opening a new research direction and demonstrating its potential as an exceptionally promising solution for high-precision and robust aerial navigation under realistic operational conditions.

In the present study, we adopt this novel adaptive control strategy for quadrotor systems, seamlessly integrating Extremum Seeking Control (ESC) with Sliding Mode Control (SMC) to autonomously and continuously fine-tune PID parameters. Within this SMESC framework, the controller gains are dynamically adjusted through the minimization of a cost function, where ISE is explicitly selected as the preferred performance metric. This choice is grounded in the comparative analysis reported in [19], which demonstrated that ISE yields the most favorable fitness values for roll, pitch, yaw, and thrust among the commonly employed indices. Concurrently, the sliding mode component guarantees robust adaptation in the presence of disturbances and modeling uncertainties. This synergistic design aims to maximize trajectory tracking accuracy, reduce steady-state error, and ensure resilient stability under realistic and dynamically varying operating conditions.

The remainder of this study is organized as follows. Section 2 presents the dynamic modeling of the quadrotor system along with the structure of the baseline PID controller. Section 3 details the proposed SMESC method and presents a rigorous stability analysis. Section 4 presents the simulation results, wherein the proposed SMESC methodology is systematically compared with Particle Swarm Optimization (PSO) PID-based approaches. Additionally, a comprehensive robustness assessment is conducted to rigorously demonstrate the superiority and validity of the proposed approach under varying operating conditions. Finally, Section 5 concludes the paper by offering key insights and outlining potential avenues for future research.

2. Dynamic Modeling of Quadrotor

The complex, nonlinear dynamics of quadrotor unmanned aerial vehicles (UAVs) pose significant challenges to the design of effective control systems [51]-[53]. These aerial platforms are inherently underactuated, exhibit strongly interconnected between translational and rotational dynamics, and remain highly susceptible to environmental disturbances. Consequently, precise and high-fidelity dynamic modeling is a prerequisite for the development of reliable and robust controllers.

In practical control applications, simplified quadrotor models are often preferred. These reduced-order representations retain the essential dynamic behavior of the system while significantly mitigating computational complexity, thereby enabling more efficient simulation, controller design, and parameter tuning. As emphasized in [54] and [2], such models constitute a valuable intermediate step, providing a rigorous platform for preliminary validation of control strategies before their deployment in more sophisticated or physically constrained environments.

2.1. Concept, Reference Frames, and Equations of Motion

The quadrotor's system framework studied here is shown in Fig. 1. It shows the two reference frames used in this work [55]. The left sketch is the inertial frame (x, y, z); the right sketch is the body-fixed frame (x^b, y^b, z^b) attached to the vehicle's center of mass, where x^b points forward, y^b to starboard, and z^b upward. Rotors are numbered counterclockwise as viewed from above; rotors 1 and 3 spin clockwise, whereas rotors 2 and 4 spin counterclockwise. Each rotor generates an upward thrust force f_i along $+z^b$. The system has twelve state variables, defined as.

$$X = \begin{bmatrix} x & \dot{x} & y & \dot{y} & z & \dot{z} & \phi & \dot{\phi} & \theta & \dot{\theta} & \psi & \dot{\psi} \end{bmatrix}^T \tag{1}$$

where y and z are inertial coordinates, $\dot{x}$, $\dot{y}$ and $\dot{z}$ are linear velocities, and ϕ, θ, ψ with their derivatives are roll, pitch, and yaw states.

Using the Newton–Euler formalism and the simplifications of [56], we get the following translational dynamics:

$$\ddot{x} = \frac{\cos\phi \sin\theta \cos\psi + \sin\phi \sin\psi}{m} U_1 \tag{2}$$

$$\ddot{y} = \frac{c\cos\phi \sin\theta \cos\psi - \sin\phi \sin\psi}{m} U_1 \tag{3}$$

$$\ddot{z} = -g + \frac{\cos\phi \cos\theta}{m} U_1 \tag{4}$$

And the rotational equations:

$$\ddot{\phi} = \frac{(I_y - I_z)\dot{\theta}\dot{\psi} - J_r\dot{\theta}\Omega + lU_2}{I_x} \tag{5}$$

$$\ddot{\theta} = \frac{(I_z - I_x)\dot{\phi}\dot{\psi} + J_r\dot{\phi}\Omega + lU_3}{I_y} \tag{6}$$

$$\ddot{\psi} = \frac{(I_x - I_y)\dot{\phi}\dot{\theta} + U_4}{I_z} \tag{7}$$

Here m is the mass, g gravity, I_x, I_y, I_z the principal inertias, J_r the total rotor inertia, and l the arm length.

The input signal U_1corresponds to the total thrust generated by the rotors, while U_2, U_3, and U_4 represent the control moments for pitch, roll, and yaw, respectively. Here, m denotes the mass of the quadrotor, $J_r$is the rotor inertia, and I_x, I_y, and I_z are the moments of inertia along the x, y, and z axes, respectively. The control input vector $U = [U_1 \quad U_2 \quad U_3 \quad U_4]^T$ is related to the rotor angular velocities Ω_i through.

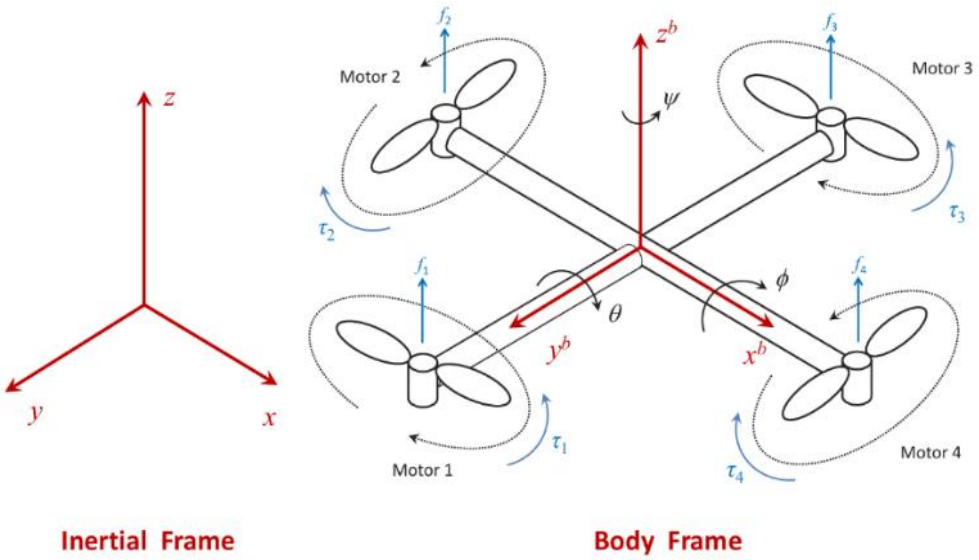

Fig. 1. Quadrotor degrees freedom [55]

$$U_1 = b(\Omega_1^2 + \Omega_2^2 + \Omega_3^2 + \Omega_4^2) \tag{8}$$

$$U_2 = bl(\Omega_4^2 - \Omega_2^2) \tag{9}$$

$$U_3 = bl(\Omega_1^2 - \Omega_3^2) \tag{10}$$

$$U_4 = d(-\Omega_1^2 + \Omega_2^2 - \Omega_3^2 + \Omega_4^2) \tag{11}$$

With the net drag-torque term:

$$\Omega = (-\Omega_1^2 + \Omega_2^2 - \Omega_3^2 + \Omega_4^2) \tag{12}$$

where b is the thrust coefficient and d the drag-torque coefficient.

These equations provide a compact yet sufficiently accurate model for subsequent controller design; a detailed derivation is available in [57].

2.2. PID Controller Design

As detailed by [56], the classical three-term or PID controller forms its command signal from three weighted components of the tracking error $e(t)$ is the instantaneous error, its time integral, and its time derivative. Mathematically:

$$u(t) = k_p e(t) + k_i \int_0^t e(\tau)\, d\tau + k_d \frac{de(t)}{dt} \tag{13}$$

where $e(t)$ is the difference between desired and measured states, k_p, k_i and k_d are the proportional, integral, and derivative gains, respectively.

For a quadrotor, this architecture is applied in six independent single-input/single-output (SISO)loops: three inner-loop controllers stabilize the attitude angles ϕ, θ and ψ, while three outer-loop controllers regulate the translational positions along the inertial x, y and z axes. The control hierarchy, therefore, begins by balancing ϕ, θ and ψ; once the vehicle is stably oriented, the outer loops adjust that attitude set points to track the desired position commands. This six-loop cascade provides a transparent framework for the SMESC algorithm to adapt k_p, k_i and k_d online, enhancing robustness under changing flight conditions.

3. Sliding Mode Extremum Seeking Controller Design

Extremum Seeking Control (ESC) is an adaptive and model-free optimization technique that iteratively perturbs a tunable parameter vector ϑ to minimize (or maximize) a measurable performance index $J(\vartheta)$. Its primary advantage lies in its ability to perform real-time optimization without requiring explicit knowledge of the system dynamics. In parallel, Sliding-Mode Control (SMC) introduces a discontinuous control law designed to drive the closed-loop system trajectory toward a predefined sliding manifold within finite time and to maintain it there despite the presence of bounded disturbances and model uncertainties.

The Sliding Mode Extremum Seeking Control (SMESC) framework effectively unifies these two complementary concepts. Within this hybrid structure, ESC is responsible for online performance optimization, while the sliding-mode mechanism ensures rapid convergence, robustness, and insensitivity to external perturbations. By combining adaptive optimization with robust control enforcement, SMESC offers a powerful and resilient tuning strategy suitable for nonlinear and uncertain systems.

Fig. 2 illustrates the block diagram of the proposed Sliding Mode Extremum Seeking Control (SMESC) scheme for a quadrotor. Independent SMESC loops are employed for the Roll, Pitch, Yaw, and Altitude axes to automatically tune the corresponding PID controller parameters, enabling decentralized and coupling-free optimization of the quadrotor dynamics.

For a given axis, the adjustable parameter vector θrepresents the PID gains to be optimized. The performance of the closed-loop system is evaluated through an objective function $J(\vartheta)$, constructed

from the corresponding tracking error and its derivatives. The output $J(\vartheta)$ is compared with an auxiliary signal $g(t)$, generated by integrating a constant negative drift $-\rho$, to form the sliding variable $S(t)$.

The sliding signal $S(t)$is then processed by a nonlinear modulation term K_θ sign[sin $(\pi S/\beta)$], which introduces a bounded periodic excitation embedded within a sliding mode structure. This mechanism enables a robust and model-free estimation of the gradient of the cost function, even in the presence of uncertainties, external disturbances, and measurement noise.

The resulting signal is integrated to update the PID gains in real time, driving the cost function toward its minimum. Once the sliding condition is reached, the system operates in a quasi-sliding mode, ensuring smooth adaptation of the PID parameters and improved tracking performance for all quadrotor motion axes, including Roll, Pitch, Yaw, and Altitude.

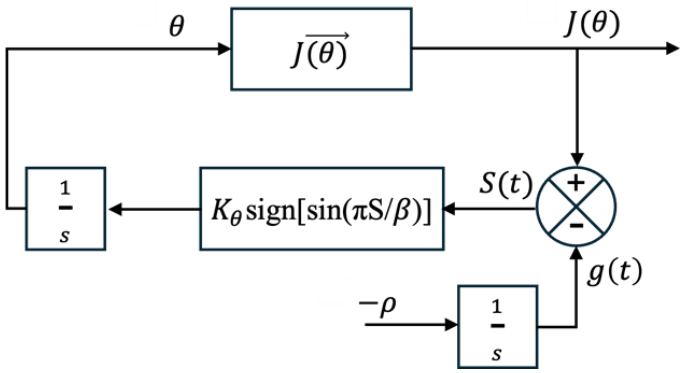

Fig. 2. Proposed block diagram of the sliding mode extremum seeking control

Fig. 3 illustrates the saturation function sat(S,β) employed in the Sliding Mode Extremum Seeking Control (SMESC) scheme [58]. The function introduces a boundary layer of width 2β around the sliding surface $S = 0$, enabling a smooth transition between the linear and saturated regions. which ensures continuous control action and mitigates chattering effects.

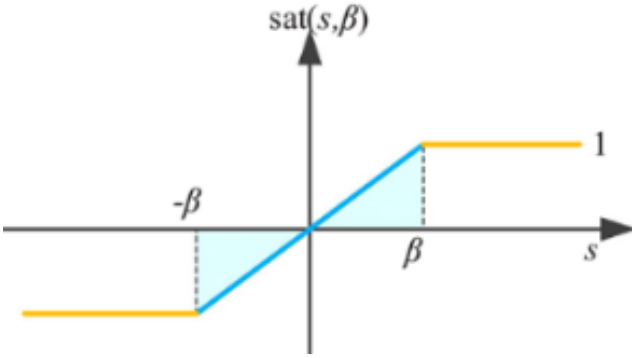

Fig. 3. The model sliding layer [59]

When $|\ S\ | > \beta$, the function saturates at ± 1, preserving the robustness properties of sliding mode control. In our approach, this saturation mechanism allows smooth online tuning of the PID gains for each axis (Roll, Pitch, Yaw, and Altitude) once the system trajectories enter the boundary layer. Consequently, the SMESC algorithm operates as a continuous extremum-seeking adaptation law near the optimum while maintaining robustness against disturbances and modeling uncertainties outside the boundary layer.

3.1. Performance Index and Sliding Variable

The dynamic behavior of a single PID loop is entirely governed by its gain vector:

$$\vartheta = [K_p, K_i, K_d]^T \tag{14}$$

where K_p, K_i, and K_d denote the proportional, integral, and derivative gain vectors, respectively. Each vector contains the corresponding gains $k_p(t)$, $k_i(t)$, and $k_d(t)$associated with the controlled axes (roll, pitch, yaw, and thrust).

To assess the controller performance, the normalized Integral Squared Error (ISE) is adopted, as it has been demonstrated to yield the most favorable fitness cost values for roll, pitch, yaw, and thrust when compared to other commonly used performance criteria. The performance index is defined as

$$J(\vartheta) = \frac{1}{t_f - t_0}\int_{t_0}^{t_f} e^2(t, \vec{\vartheta})dt \tag{15}$$

Where $e(t, \vec{\vartheta}) = r(t) - y(t, \vec{\vartheta})$ is the tracking error between reference $r(t)$ and closed-loop output $y(t)$.

The goal is to reach

$$\begin{cases} \vartheta_{\min} = \arg\min_{\theta} J(\vartheta), \\ J_{\min} = J(\vartheta_{\min}) \end{cases} \tag{16}$$

To impose a sliding-mode structure, we define a sliding surface

$$S(t) = J(\vartheta) - g(t) \tag{17}$$

with the auxiliary signal

$$\begin{cases} \dot{g}(t) = -\rho, \quad \rho > 0 \\ g(0) = J(\vartheta_0) \end{cases} \tag{18}$$

Thus, $g(t)$ is a ramp that progressively descends along the cost axis, while the surface $S = 0$ defines the locus where the real-time cost precisely tracks and remains aligned with this dynamically moving target.

3.2. Parameter-Update Law and Stability Analysis

The classical ESC tuner updates the gain vector ϑ with a pure sign operator, which can induce severe chattering. Following [39], [58], we replace sign(.) by sliding-layer saturation:

$$\text{sat}(S, \beta) = \begin{cases} 1, & S > \beta \\ \dfrac{S}{\beta}, & |S| \le \beta \\ -1, & S < -\beta \end{cases} = \begin{cases} \text{sign}(S) & |S| > \beta \\ \dfrac{S}{\beta} & |S| \le \beta \end{cases} \tag{19}$$

Thus, the control law adopts high-gain behavior outside the boundary layer $|S| > \beta$and transitions to a linear response within it, seamlessly combining the inherent robustness of sliding-mode control with the smooth, adaptive characteristics of ESC. The complete parameter-update rule is then formulated as follows:

$$\dot{\vartheta} = K_\vartheta \text{sat}(S/\beta), \qquad K_\vartheta = \text{diag}(K_p, K_i, K_d) > 0 \tag{20}$$

The analysis presented in [58] demonstrates that the closed-loop system admits multiple candidate sliding surfaces. Accordingly, a reachability condition is established to guarantee convergence toward the cost-minimizing surface. To this end, we consider the following Lyapunov-like function.

$$V = \frac{1}{2}S^2 \tag{21}$$

Using the definitions given in (19) and (20), the time derivative of the Lyapunov function in (21), evaluated along the SMESC trajectories, can be expressed as follows [59].

$$\dot{V} = S\dot{S} = S\left(\frac{\partial J(\vartheta)}{\partial \vartheta}\dot{\vartheta} + \rho\right) \tag{22}$$

with the cost-gradient vector

$$\psi_s(\vartheta) = \frac{\partial J(\vartheta)}{\partial \vartheta} \tag{23}$$

Substituting $\dot{\vartheta}$ and $\mathrm{sat}(S/\beta)$ in (22) gives:

$$\dot{V} = -K_\vartheta \psi_s(\vec{\theta})\mathrm{sat}(S/\beta)J(\vec{\vartheta})S + \rho S \tag{24}$$

Outside the boundary layer ($|S| \le \beta$), the saturation reduces to $\mathrm{sign}(S)$; hence:

$$\dot{V} = (-K_\vartheta |\psi_s(\vec{\vartheta})|J(\vec{\vartheta}) + \rho)|S| \tag{25}$$

A sufficient condition for $\dot{V} < 0$ is therefore:

$$|\psi_s(\vec{\vartheta})|J(\vec{\vartheta}) > \frac{\rho}{K_\vartheta} \tag{26}$$

which guarantees that S decreases monotonically until it enters the layer $|S| \le \beta$.

Assume (26) holds, the condition on the derivative of the Lyapunov function satisfies

$$\dot{V} \le -k_s|S| \tag{27}$$

with:

$$k_s = K_\vartheta|\psi_s(\vec{\vartheta})|J(\vec{\vartheta}) - \rho > 0 \tag{28}$$

Because of equation (21) (leading to $|S| = \sqrt{2V}$), we have:

$$\dot{V} < -k_s\sqrt{2V} \tag{29}$$

so $V(t)$ (hence, $S(t)$) reaches zero in finite time t_s, with:

$$t_s = \sqrt{2V(0)}/k_s \tag{30}$$

Once $|S| \le \beta$ the saturation becomes linear; chattering is eliminated, and the tuner behaves like a smooth extremum-seeking gradient descent that drives $J(\vartheta)$ toward its minimum. If condition (28) is not met on a particular sliding surface, the system drifts away until it encounters another surface where (28) is satisfied, as shown in [58]-[60]. By selecting K_ϑ, ρ, and β such that (28) is fulfilled over the expected parameter range, SMESC achieves robust finite-time convergence while continuously optimizing the PID gains.

The proposed SMESC algorithm is used to adaptively tune the PID controller gains in real time. Based on the extremum seeking principle combined with sliding mode adaptation, the algorithm continuously updates the PID parameters K_p, K_i, and K_d in order to minimize the tracking error between the reference and the system output. The measured outputs of the quadrotor $(\phi, \theta, \psi, z)$are fed back to the SMESC block, which adjusts the controller gains online to improve tracking performance and robustness against disturbances and model uncertainties.

Fig. 4 is the block diagram of the proposed SMESC-based PID control architecture for a quadrotor. Each motion axis-Roll (ϕ), Pitch (θ), Yaw (ψ), and Altitude (z)-is controlled by an independent PID loop tuned online using the Sliding Mode Extremum Seeking Control (SMESC) algorithm. The SMESC module continuously adjusts the PID gains to optimize tracking performance in the presence of disturbances and model uncertainties. Feedback from the quadrotor's sensors is used to compute the control error for each axis, which is then fed into the corresponding SMESC-PID loop for real-time adjustment.

Algorithm 1: SMESC-Based PID Tuning for a Quadrotor

Initialization:;
Initialize PID gains K_p, K_i, K_d for each loop: Roll (ϕ), Pitch (θ), Yaw (ψ), Altitude (z);
Initialize sliding surface parameters: slope λ, boundary layer width β;
Initialize ESC parameters: perturbation amplitude a, adaptation gain γ;
Define reference signal $r(t)$;
Define performance cost function: $J(\theta)$;
while system is operating **do**
    // Error Computation
    Measure quadrotor outputs $y(t)$;
    Compute tracking error: $e(t) = r(t) - y(t)$;
    // Sliding Surface (SMESC)
    Compute sliding surface $S(t)$;
    Apply boundary layer $\text{sat}(S/\beta)$ to reduce chattering;
    // Extremum Seeking -- Cost Evaluation
    Evaluate $J(\theta) = \int e^2(t)\, dt$ over one excitation period;
    Estimate gradient of J : $\widehat{\nabla J}$ via demodulation and averaging of J;
    // Adaptive Gain Update
    Update PID gains via SMESC adaptive law ;
    Feed updated gains K_p, K_i, K_d back to all PID loops;
Stability Condition (Lyapunov-based):;
/* If $\dot{V} \leq -k_s|S|$ holds, the closed-loop system remains stable and the SMESC guarantees convergence of $K_p(t)$, $K_i(t)$, $K_d(t)$ to their optimal values. */

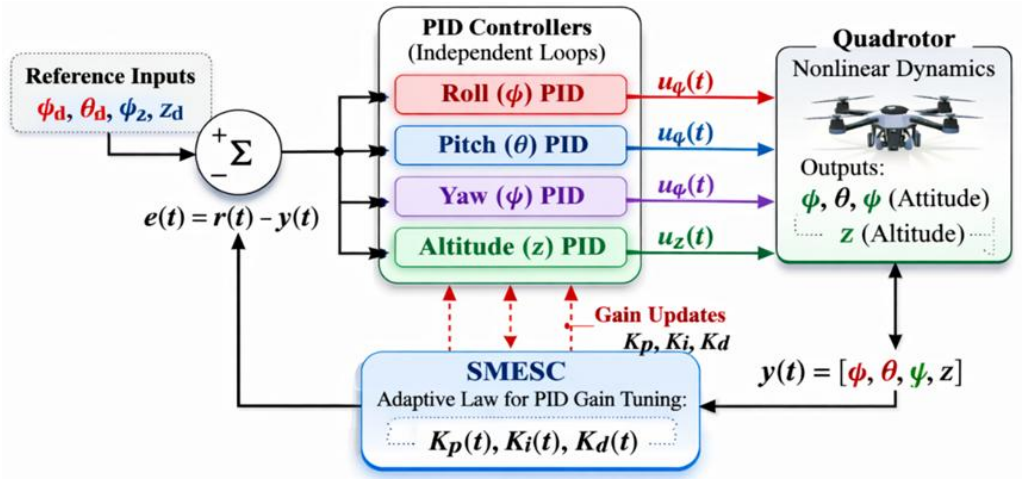

Fig. 4. Block diagram of the proposed SMESC-based PID control architecture for a quadrotor

4. Results and Discussion

This section presents MATLAB simulation results validating the proposed SMESC-tuned PID controller on the nonlinear quadrotor model described in Section 2. A comparative study with a PSO-based PID tuning method [19] is conducted using the same normalized Integral Squared Error (ISE).

In addition, the robustness and disturbance rejection performance of the proposed SMESC controller are evaluated.

4.1. Simulation Setup

The physical parameters of the virtual quadrotor are specified in Table 1 [17], while the corresponding SMESC gains, selected in accordance with the design rule (26), are summarized in Table 2.

Table 1. Physical quadrotor parameters used in simulation

Parameters	Values and Units Simulation
Time	10 sec
Mass(m)	1 Kg
Gravity (g)	9.81 m/s^2
Length of the rods (l)	0.25 m

Table 2. Controller-tuning parameters for SMESC

Parameter	Description	Value	Selection rationale
K_ϑ	SMESC adaptation gain	**0.1**	Ensures fast convergence without oscillations
β	Boundary layer width	**0.05**	Selected from worst-case axis (Altitude)
ρ	Drift coefficient	**0.02**	Guarantees monotonic decrease of (g(t))
$S(0)$	Initial sliding variable	0	Equilibrium initialization

A single set of SMESC parameters was used for all quadrotor axes (Roll, Pitch, Yaw, and Altitude). The boundary layer width β was selected based on the most demanding axis (Altitude), ensuring robust and chattering-free operation across all control loops. The smooth tracking performance observed in Fig. 5 confirms the effectiveness of this unified parameter selection.

All simulations are conducted over a 10-second horizon with a fixed sampling period of 1 ms. The inner-loop attitude PID controllers are initialized with conservative baseline gains, identical to those adopted in [21], and are subsequently allowed to adapt online through the SMESC mechanism. The outer-loop position controllers follow a cascaded architecture, receiving updated attitude set-points at a rate of 50 Hz. Sensor noise is incorporated to reflect realistic operating conditions, modeled as zero-mean Gaussian disturbances with standard deviations of 1 cm for position measurements and 0.1° for attitude signals. Fig. 4 shows the cost function ($J(\vartheta)$) reduction with time while the proposed approach is used to tune the PID parameters.

Fig. 6 presents the time-domain responses of the quadrotor under the proposed SMESC-based controller, including the roll, pitch, yaw angles, and altitude. The system outputs closely track their reference trajectories, exhibiting fast transient behavior, negligible overshoot, and near-zero steady-state error. Stable performance is maintained during reference changes, demonstrating the robustness and effectiveness of the proposed controller for both attitude and altitude regulation. The corresponding control inputs are illustrated in Fig. 7. The attitude control inputs u_1, u_2, and $u_3$are confined within $[-1,+1]$, $[-2,+2]$, and $[-0.4,+0.4]$, respectively. The altitude-related control signal u_4 remains bounded and within approximately $[-180,+180]$, ensuring reliable and stable vertical motion. These signals exhibit smooth and well-damped profiles, with noticeable variations occurring mainly during reference transitions, demonstrating the effective suppression of chattering phenomena and the absence of actuator saturation.

Overall, the bounded and well-structured control signals, combined with the high tracking accuracy observed in the system responses, confirm that the proposed SMESC controller provides robust, energy-efficient, and physically feasible control actions, making it well-suited for real-time quadrotor applications.

Table 3 presents quantitative performance metrics of the proposed SMESC-based controller. The results indicate negligible steady-state error, very low RMSE and IAE values, and zero overshoot for

all axes. Additionally, the control inputs remain bounded with moderate amplitudes, demonstrating the efficiency and robustness of the proposed control strategy.

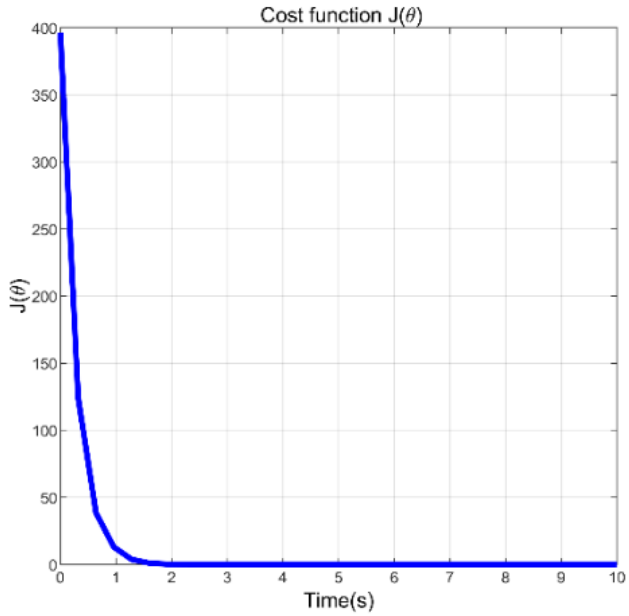

Fig. 5. The cost function ($J(\vartheta)$) reduces with time

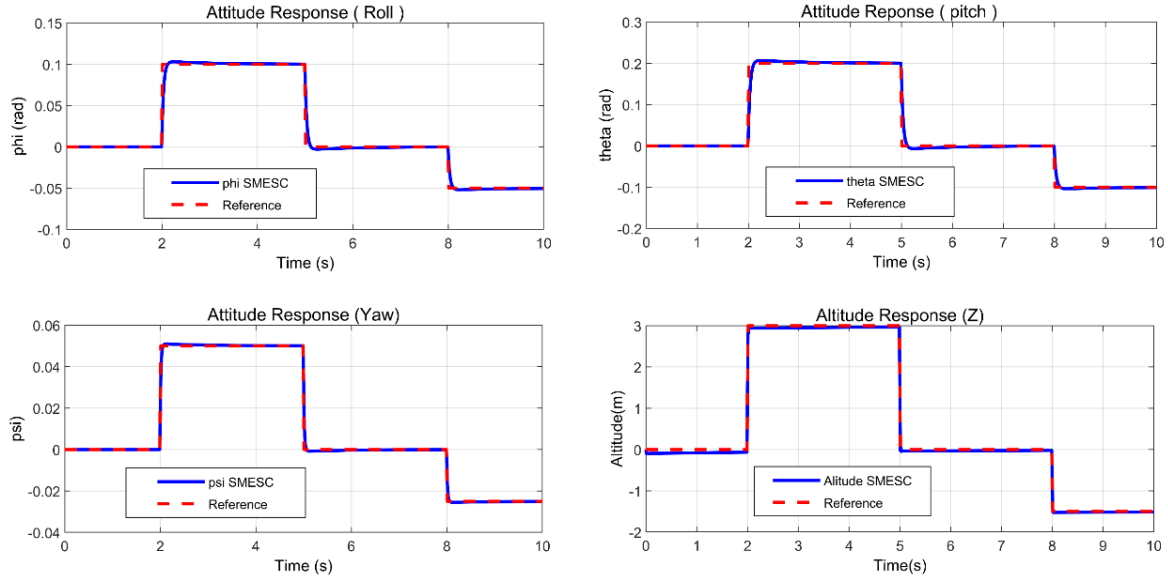

Fig. 6. Time response of roll, pitch yaw and altitude using SMESC

Table 3. Quantitative performance metrics of the proposed SMESC controller

Axis	SSE	RMSE	IAE	Overshoot (%)	Settling Time (s)	Max Control Effort
Roll φ	≈0 rad	0.002	0.004	0	≈0.30	≈0.9 N
Pitch θ	≈0 rad	0.003	0.006	0	≈0.35	≈1.9 N
Yaw ψ	≈0 rad	0.001	0.003	0	≈0.25	≈0.4 Nm
Altitude z	≈0 m	0.01	0.02	0	≈0.40	≈170 N

Where

- **SSE**: Steady-State Error
- **RMSE**: Root Mean Square Error
- **IAE**: Integral of Absolute Error

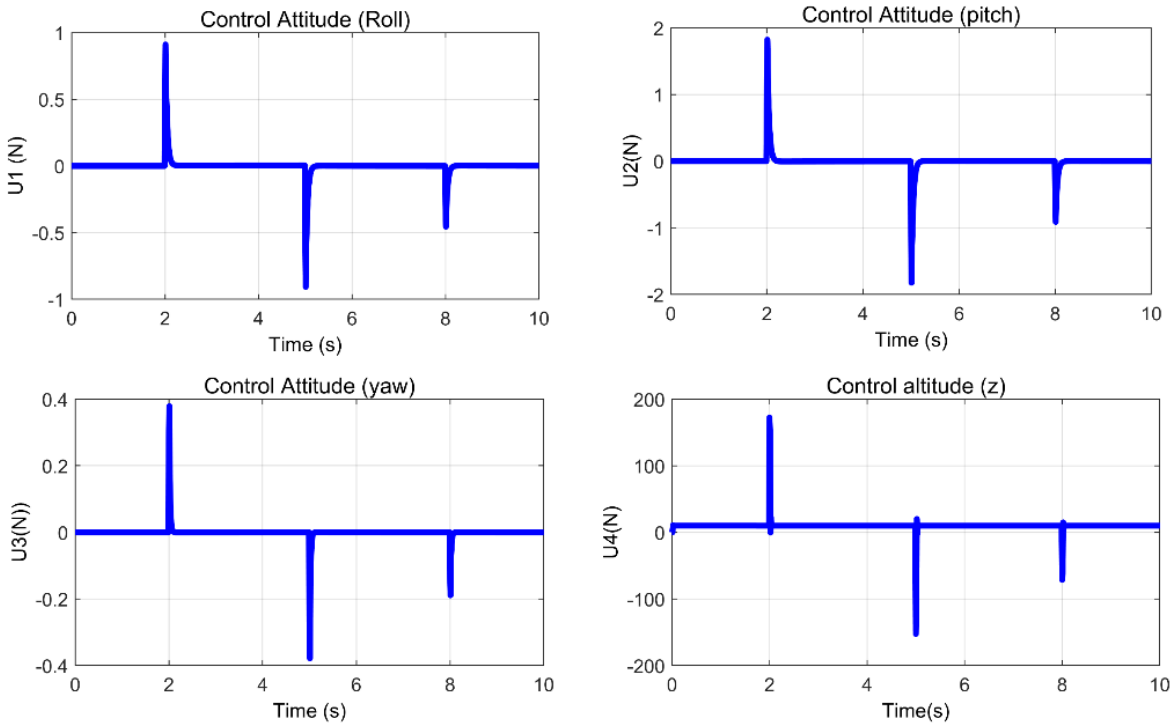

Fig. 7. Control signals for attitude (roll, pitch and yaw) and altitude (z)

4.2. Comparative Study

To ensure a fair and consistent comparison, the Particle Swarm Optimization (PSO) method [19] is introduced as a benchmark approach for PID parameter tuning alongside the proposed SMESC strategy. For both tuning methods, the same performance criterion, namely the normalized Integral Squared Error (ISE), is employed as the objective function. This choice allows an objective evaluation of the control performance under identical optimization conditions, thereby highlighting the relative advantages of the proposed SMESC-based tuning approach. Fig. 8 illustrates the comparative time responses obtained using SMESC- and PSO-based controllers. It can be observed that the SMESC approach ensures significantly faster transient behavior, with shorter rise times and settling times for all attitude angles and altitude. In addition, SMESC exhibits negligible overshoot and well-damped responses, whereas the PSO-based controller presents higher overshoot and longer settling periods. These results highlight the superiority of SMESC in terms of rapid convergence, robustness, and dynamic performance.

Table 4 strikingly highlights the superiority of the SMESC controller. Across all variables, rise times are reduced by 40–44% and settling times by 30–33% compared to the PSO-tuned controller. These improvements demonstrate faster stabilization, more efficient transient responses, and robust, precise dynamic performance, confirming SMESC as an effective solution for advanced quadrotor control.

4.3. Disturbance Rejection Performance of the Controllers

In this section, the disturbance rejection performance of the proposed SMESC-PID controller is evaluated. The simulations were conducted using the following reference values: $z = 5$ m, Roll = 5° ($\pi/36$ rad), Pitch = 5° ($\pi/36$ rad), and Yaw = 5° ($\pi/36$ rad). To assess robustness, external disturbances were introduced as additive perturbations on the system dynamics at approximately 2 s, 4 s, and 6 s. These disturbances were short impulse-like signals applied to the roll, pitch, yaw, and altitude channels, with magnitudes set to small bounded values (around 5–10% of the nominal control input) to emulate realistic perturbations such as wind gusts. Each disturbance lasted about 0.1 s, after which the system returned to nominal conditions. The corresponding system responses are shown in Fig. 9, where brief deviations can be observed before the controller rapidly restores accurate tracking.

These results demonstrate the robustness of the proposed approach, confirming that the SMESC-PID controller effectively mitigates the effects of external disturbances while maintaining stability and precise trajectory tracking.

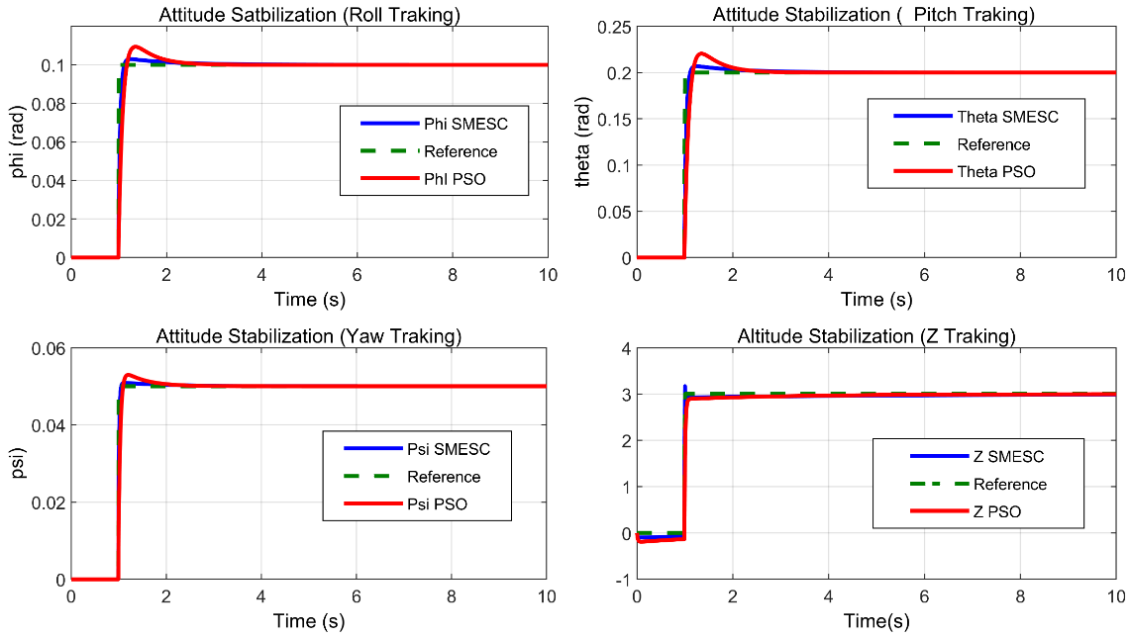

Fig. 8. Comparative time responses of SMESC and PSO controllers

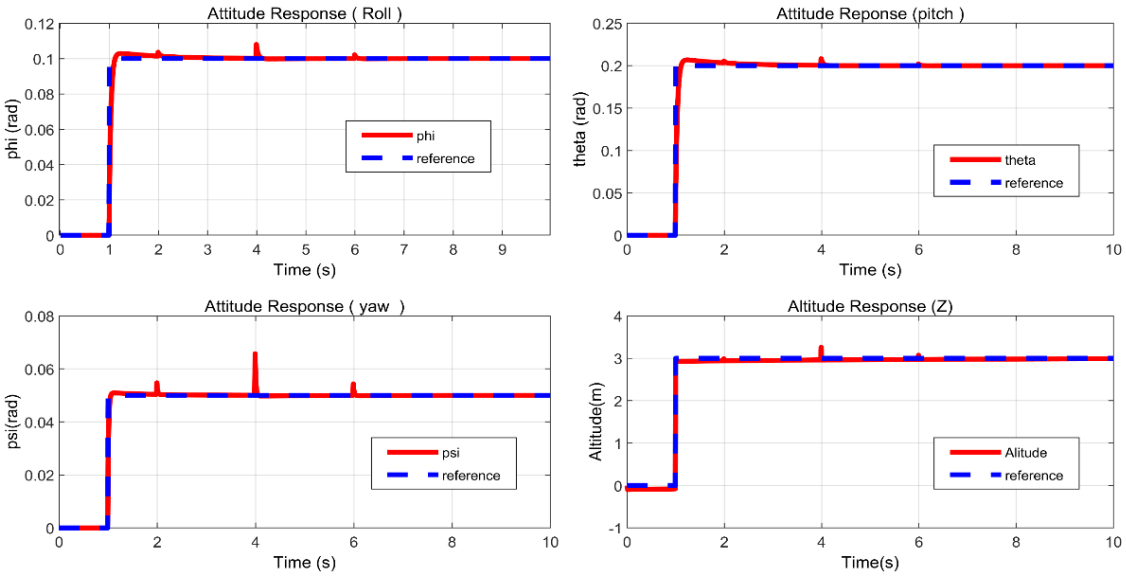

Fig. 9. Displacement results for SMESC with disturbance

Table 4. Comparative time-domain performance of SMESC and PSO controllers

Variable	Method	Rise Time (s)	Settling Time (s)	Rise Time Improvement	Settling Time Improvement
Roll φ	SMESC	0.12	1.4	≈ 40 %	≈ 30 %
	PSO	0.20	2.0		
Pitch θ	SMESC	0.13	1.5	≈ 41 %	≈ 32 %
	PSO	0.22	2.2		
Yaw ψ	SMESC	0.10	1.3	≈ 44 %	≈ 32 %
	PSO	0.18	1.9		
Altitude z	SMESC	0.15	1.6	≈ 40 %	≈ 33 %
	PSO	0.25	2.4		

5. Conclusion

This study investigates the efficacy of employing the proposed SMESC (Sliding Mode Extremum Seeking Control) optimization algorithm for tuning Proportional-Integral-Derivative (PI-D) controllers in quadrotor applications. The SMESC methodology combines the adaptive, model-free optimization capability of Extremum Seeking Control (ESC) with the inherent robustness of Sliding Mode Control (SMC), constructing a novel control strategy that benefits from the strengths of both approaches. The method was systematically developed, with a detailed construction procedure and an appropriate block diagram, while effectively eliminating the chattering commonly associated with traditional Sliding Mode Control.

Analysis reveals that the SMESC-PID controller demonstrably outperforms its counterpart, particularly the PSO-based controller, in mitigating steady-state error and improving transient performance. Quantitatively, SMESC reduces rise time by approximately 40% and settling time by about 30%, while significantly decreasing overshoot by more than 60% compared to the PSO-tuned controller under identical optimization conditions and using the same performance index. The algorithm effectively and iteratively tunes the PI-D controller's gain parameters (k, T_i, T_d), dynamically adjusting them until the quadrotor achieves the desired displacement, providing strong evidence of system stability.

Furthermore, the robustness of the SMESC-PID controller was thoroughly evaluated by introducing additive disturbances, confirming its ability to maintain stability and precise control under challenging conditions. The observed reduction in steady-state error and the success of the iterative optimization underscore the potential of SMESC-PID controllers for enhancing quadrotor performance beyond conventional optimization techniques.

Future work could explore integrating SMESC-PID controllers with advanced strategies to enhance adaptability, disturbance rejection, and flight performance. Experimental validation under varying conditions and extending the approach to multi-agent systems for coordinated autonomous missions could further expand the operational capabilities of quadrotor fleets in civilian and industrial applications.

Nevertheless, some limitations of the proposed SMESC approach should be acknowledged. The results are primarily validated through simulation, and practical implementation may be influenced by real-world constraints such as sensor noise, actuator saturation, and computational delays. Moreover, the independent axis control architecture does not explicitly account for strong cross-coupling effects during highly dynamic maneuvers.

Author Contribution: All authors contributed equally to the main contributor to this paper. All authors read and approved the final paper.

Funding: This research received no external funding.

Conflicts of Interest: The authors declare no conflict of interest.

References

[1] T. Al-husnawy and A. Al-Ghanimi, "A Review of Control Methods for Quadrotor UAV," *Kufa Journal of Engineering*, vol. 15, no. 4, pp. 98-124, 2024, https://doi.org/10.30572/2018/KJE/150408.

[2] A. Zulu and S. John, "A review of control algorithms for autonomous quadrotors," *Open Journal of Applied Sciences*, vol. 4, pp. 547-556, 2014, https://doi.org/10.4236/ojapps.2014.414053.

[3] D. Kotaski, Z. Benic, and M. Krzenar, "Control design for unmanned aerial vehicles with four rotors," *Interdisciplinary Description of complex systems*, vol. 14, no. 2, pp. 236-245, 2016, https://doi.org/10.7906/indecs.14.2.12.

[4] F. M. B. Lima, Á. M. Bueno, and P. S. Silva, "Modeling, Construction and Control of Quadrotors," *Vibration Engineering and Technology of Machinery: Proceedings of VETOMAC XV 2019*, 2021, https://doi.org/10.1007/978-3-030-60694-7_16.

[5] B. Acar. *Robust Nonlinear Model Predictive Control for Quadrotor Collision Avoidance with Interacting Multiple Model-Based Obstacle Motion Prediction*. East Technical University ProQuest Dissertations & Theses, Turkey, 2025, https://www.proquest.com/docview/3261944328?fromopenview=true&pq-origsite=gscholar&sourcetype=Dissertations%20&%20Theses.

[6] I. B. Ghiloubi, L. Abdou, and O. Lahmar, "Anti-Collision Formation Control for Drone Swarms Tracking Aerial Targets Under Wind Disturbance," *International Journal of Robotics and Control Systems*, vol. 5, no. 6, pp. 2831-2852, 2025, https://pubs2.ascee.org/index.php/IJRCS/article/view/1994.

[7] P. Bouffard. *On-board Model Predictive Control of a Quadrotor Helicopter: Design, Implementation, and Experiments*. Univ. of California, 2012, https://apps.dtic.mil/sti/html/tr/ADA572108/.

[8] Y. Zhou, "Robust Nonlinear Model Predictive Control for Quadrotor UAV Trajectory Tracking," *2nd International Conference on Mechanics, Electronics Engineering and Automation (ICMEEA 2025)*, pp. 864-877, 2025, https://doi.org/10.2991/978-94-6463-821-9_83.

[9] R. Mahony, Vijay Kumar and Peter Corke, "Multirotor Aerial Vehicles: Modeling, Estimation, and Control of Quadrotor," *IEEE Robotics & Automation Magazine*, vol. 19, no. 3, pp. 20-30, 2012, https://doi.org/10.1109/MRA.2012.2206474.

[10] O. Bouaiss, R. Mechgoug, and R. Ajgou, "Modeling, Control and Simulation of Quadrotor UAV," *2020 1st International Conference on Communications, Control Systems and Signal Processing (CCSSP)*, pp. 340-345, 2020, https://doi.org/10.1109/CCSSP49278.2020.9151687.

[11] N. Basil *et al*., "Multi-criteria decision model for multicircular flight control of unmanned aerial vehicles through a hybrid approach," *Scientific Reports*, vol. 15, no. 1, 2025, https://doi.org/10.1038/s41598-025-01508-y.

[12] H. M. Marhoon *et al*., "Metaheuristic-driven optimisation of support vector regression models for precision control in unmanned aerial vehicle systems," *Buletin Ilmiah Sarjana Teknik Elektro*, vol. 7, no. 3, pp. 608–624, Oct 2025, https://journal2.uad.ac.id/index.php/biste/article/view/14251.

[13] F. R. T. Hasan and S. A. Akbar, "PID control tuning based on wind speed sensor in flying robot," *Control Systems and Optimization Letters*, vol. 1, no. 3, pp. 151-156, 2023, https://doi.org/10.59247/csol.v1i3.56.

[14] N. H. Sahrir and M. A. M. Basri, "Modelling and Manual Tuning PID Control of Quadcopter," in *Control, Instrumentation and Mechatronics: Theory and Practice*, pp. 346-357, 2022, https://doi.org/10.1007/978-981-19-3923-5_30.

[15] R. P. Borase, D. K. Maghade, S. Y. Sondkar, and S. N. Pawar, "A review of PID control, tuning methods and applications," *International Journal of Dynamics and Control*, vol. 9, pp. 818–827, 2021, https://doi.org/10.1007/s40435-020-00665-4.

[16] N. Ramadhani, A. Ma'arif, and A. Çakan, "Implementation of PID control for angular position control of Dynamixel servo motor," *Control Systems and Optimization Letters*, vol. 2, no. 1, pp. 8-14, 2024, https://doi.org/10.59247/csol.v2i1.40.

[17] M. A. M. Basri, A. R. Husain, and K. A. Danapalasingam, "Stabilization and trajectory tracking control for underactuated quadrotor helicopter subject to wind-gust disturbance," *Sadhana*, vol. 40, no. 5, pp. 1531-1553, 2015, https://doi.org/10.1007/s12046-015-0384-4.

[18] I. Lopez-Sanchez and J. Moreno-Valenzuela, "PID control of quadrotor UAVs: A survey," *Annual Reviews in Control*, vol. 56, p. 100900, 2023, https://doi.org/10.1016/j.arcontrol.2023.100900.

[19] N. H. Sahrir and M. A. M. Basri, "Index performance comparison PSO–PID controller for quadcopter UAV," *Arabian Journal for Science and Engineering*, vol. 48, no. 2, pp. 1-15, 2023, https://doi.org/10.1007/s13369-023-08088-x.

[20] A. Sheta, M. Braik, D. R. Maddi, A. Mahdy, S. Aljahdali, and H. Turabieh, "Optimization of PID controller to stabilize quadcopter movements using meta-heuristic search algorithms," *Applied Sciences*, vol. 11, no. 14, p. 6492, 2021, https://doi.org/10.3390/app11146492.

[21] A. M. Ahmad, R. A. Yauri, and M. I. Kamba, "Trajectory Optimization of Quadrotor-UAV Drone Using Genetic Algorithm," *Equity Journal of Science and Technology*, vol. 8, no. 1, p. 95, 2022, https://doi.org/10.4314/equijost.v8i1.16.

[22] M. K. Kurnaz, Y. Ölmez, and G. O. Koca, "Altitude Control of Quadrotor Based on Metaheuristic Methods," *International Journal of Innovative Engineering Applications*, vol. 9, no. 1, pp. 37-46, 2025, https://doi.org/10.46460/ijiea.1564844.

[23] I. B. Ghiloubi1, L. Abdou, O. Lahmar, and A. H. Drid, "Quadrotor Trajectory Tracking Under Wind Disturbance Using Backstepping Control Based on Different Optimization Techniques," in *The 5th International Electronic Conference on Applied Sciences*, vol. 87, no. 1, p. 93, 2024, https://doi.org/10.3390/engproc2025087093.

[24] G. Airlangga, "Advancing UAV path planning system: A software pattern language for dynamic environments," *Buletin Ilmiah Sarjana Teknik Elektro*, vol. 5, no. 4, pp. 475–497, Dec 2023, https://doi.org/10.12928/biste.v5i4.9407.

[25] B. Bekhiti, K. Hariche, A. Ma'arif, and A. Sharkawy, "A Nonlinear Automatic Control Strategy for Autopiloting a Fourth-Generation Combat Aircraft: The Soukhoï Su-30," *International Journal of Robotics and Control Systems*, vol. 5, no. 6, pp. 2957-2994, 2025, https://pubs2.ascee.org/index.php/IJRCS/article/view/2169.

[26] A. Israr, Z. A. Ali, E. H. Alkhammash, and J. J. Jussila, "Optimization Methods Applied to Motion Planning of Unmanned Aerial Vehicles: A Review," *Drones*, vol. 6, no. 5, p. 126, 2022, https://doi.org/10.3390/drones6050126.

[27] S. M. Raafat and Z. S. Mahmoud, "Robust Multiple Model Adaptive Control for Dynamic Positioning of Quadrotor Helicopter System," *Engineering and Technology Journal*, vol. 36, pp. 1249-1259, 2018, https://doi.org/10.30684/etj.36.12A.6

[28] A. N. Muhsen and S. M. Raafat, "Optimized PID control of quadrotor system using extremum seeking algorithm," *Engineering and Technology Journal*, vol. 39, no. 6, pp. 996–1010, 2021, https://doi.org/10.30684/etj.v39i6.1850.

[29] M. Krstić and H.-H. Wang, "Stability of extremum seeking feedback for general nonlinear dynamic systems," *Automatica*, vol. 36, no. 4, pp. 595–601, 2000, https://doi.org/10.1016/S0005-1098(99)00183-1.

[30] Y. Zhu and E. Fridman, "A Time-delay Approach for Extremum Seeking of Nonlinear Static Maps," *IFAC-PapersOnLine*, vol. 56, no. 1, pp. 258-263, 2023, https://doi.org/10.1016/j.ifacol.2023.02.044.

[31] S. M. Raafat, A. N. Muhsen, and A. A. A. Alawsai, "Extremum Seeking Based PID Control of Quadrotor System," *Mobile Robot: Motion Control and Path Planning*, pp. 609–642, 2023, https://doi.org/10.1007/978-3-031-26564-8_17.

[32] M. Krstić, "Performance improvement and limitations in extremum seeking control," *Systems & Control Letters*, vol. 39, no. 5, pp. 313-326, 2000, https://doi.org/10.1016/S0167-6911(99)00111-5.

[33] M. Herrera, W. Chamorro, A. P. Gómez, and O. Camacho, "Sliding Mode Control: An Approach to Control a Quadrotor," *2015 Asia-Pacific Conference on Computer Aided System Engineering*, pp. 314-319, 2015, https://doi.org/10.1109/APCASE.2015.62.

[34] N. Ahmed and M. Chen, "Sliding mode control for quadrotor with disturbance observer," *Advances in Mechanical Engineering*, vol. 10, no. 7, 2018, https://doi.org/10.1177/1687814018782330.

[35] J. Pan, B. Shao, J. Xiong and Q. Zhang, "Attitude control of quadrotor UAVs based on adaptive sliding mode," *International Journal of Control, Automation and Systems*, vol. 21, p. 2698–2707, 2023, https://doi.org/10.1007/s12555-022-0189-2.

[36] B. Zheng, Y. Wu, and Z. Chen, "Adaptive Sliding Mode Attitude Control of Quadrotor UAVs Based on the Delta Operator Framework," *Dynamical Systems: Theory and Applications*, vol. 14, no. 3, p. 498, 2022, https://doi.org/10.3390/sym14030498.

[37] B. Li and X. Zhao, "Neural Network-Based Adaptive Sliding Mode Control for T-S Fuzzy Fractional Order Systems," in *IEEE Transactions on Circuits and Systems II: Express Briefs*, vol. 70, no. 12, pp. 4549-4553, Dec. 2023, https://doi.org/10.1109/TCSII.2023.3289988.

[38] N. Basil, H. M. Marhoon, D. F. Sahib, A. F. Mohammed, H. M. Ridha, and A. Ma'arif, "Accelerated black hole optimization algorithm with enhanced FOPID controller for omni-wheel drive mobile robot system," *Neural Computing and Applications*, vol. 37, no. 21, pp. 16983–17014, 2025, https://doi.org/10.1007/s00521-025-11310-6.

[39] Q. Cao *et al*., "An improved sliding mode control based on fuzzy logic for quadrotor unmanned aerial vehicles under unmatched uncertainty," *Frontiers of Information Technology and Electronic Engineering*, vol. 26, no. 10, pp. 1942–1953, 2025, https://doi.org/10.1631/FITEE.2500058.

[40] A. H. Sanchez, A. Poznyak, and I. Chairez, "Extremum seeking control for the trajectory tracking of a skid steering vehicle via averaged sub-gradient integral sliding-mode theory," *Robotics and Autonomous Systems*, vol. 174, p. 104609, 2024, https://doi.org/10.1016/j.robot.2023.104609.

[41] Y. Pan and Ü. Özgüner, "Extremum Seeking Control with Sliding Mode," *IFAC Proceedings Volumes*, vol. 35, no. 1, pp. 371-376, 2002, https://doi.org/10.3182/20020721-6-ES-1901.00311.

[42] Y. B. Salamah and Ü. Özgüner, "Sliding Mode Multivariable Extremum Seeking Control with Application to Wind Farm Power Optimization," *2018 Annual American Control Conference (ACC)*, pp. 5321-5326, 2018, https://doi.org/10.23919/ACC.2018.8431180.

[43] Z. Zhao, S. Song, Y. Dong and L. Li, "Extremum Seeking Based on Sliding Mode Control for Precision Motion Systems," *2024 36th Chinese Control and Decision Conference (CCDC)*, pp. 4041-4046, 2024, https://doi.org/10.1109/CCDC62350.2024.10587502.

[44] Y. Pan, K. D. Kumar and G. Liu, "Extremum seeking control with second-order sliding mode," *SIAM Journal on Control and Optimization*, vol. 50, no. 6, pp. 3447–3469, 2012, https://doi.org/10.1137/090778481.

[45] L. L. Fu and Ü. Özgüner, "Variable structure extremum seeking control based on sliding mode gradient estimation for a class of nonlinear systems," in *Proc. American Control Conf. (ACC)*, pp. 8-13, 2009, https://doi.org/10.1109/ACC.2009.5160207.

[46] O. Bourebia, "Stabilizing constrained control for discrete-time multivariable linear systems via positive polyhedral invariant sets," in *SCRS Conference Proceedings on Intelligent Systems*, pp. 231-237, 2022, https://doi.org/10.52458/978-93-91842-08-6-22.

[47] O. Bourebia, "A Stable and Admissible Explicit Solution to Fuzzy Predictive Control using polyhedral invariant sets," *2023 International Conference on Electrical Engineering and Advanced Technology (ICEEAT)*, pp. 1-6, 2023, https://doi.org/10.1109/ICEEAT60471.2023.10426296.

[48] Y. Pan, Ü. Özgüner, and T, Acarman, "Stability and performance improvement of extremumseeking controlwith sliding mode," *International Journal of Control*, vol. 76, no. 9-10, pp. 968–985, 2003, https://doi.org/10.1080/0020717031000099100.

[49] C. Jui-Ho, H.-T. Yau, and W. Hung, "Design and Study on Sliding Mode Extremum Seeking Control of the Chaos Embedded Particle Swarm Optimization for Maximum Power Point Tracking in Wind Power Systems," *Energies*, vol. 7, no. 3, pp. 1706-1720, 2014, https://doi.org/10.3390/en7031706.

[50] H. A. Trinh *et al*., "Robust adaptive control strategy for a bidirectional DC-DC converter based on extremum seeking and sliding mode control," *Sensors*, vol. 23, no. 1, p. 457, 2023, https://doi.org/10.3390/s23010457.

[51] Y. Naidoo, R. Stopforth, and G. Bright, "Quadrotor unmanned aerial vehicle helicopter modelling & control," *International Journal of Advanced Robotic Systems*, vol. 8, no. 4, pp. 139-149, 2011, https://doi.org/10.5772/45710.

[52] M. Idrissi and F. Annaz, "Dynamic Modelling and Analysis of a Quadrotor Based on Selected Physical Parameters," *International Journal of Mechanical Engineering and Robotics Research*, vol. 9, no. 6, pp. 784-790, 2020, https://doi.org/10.18178/ijmerr.9.6.784-790.

[53] M. Walid, N. Slaheddine, A. Mohamed, and B. Lamjed, "Modeling and control of a quadrotor UAV," *2014 15th International Conference on Sciences and Techniques of Automatic Control and Computer Engineering (STA)*, pp. 343-348, 2014, https://doi.org/10.1109/STA.2014.7086762.

[54] T. Dief, A. H. Kassem, and G. M. El Baioumi, "Modeling and Attitude Stabilization of Indoor Quad Rotor," *International Review of Aerospace Engineering (IREASE)*, vol. 7, no. 2, 2014, https://doi.org/10.15866/irease.v7i2.783.

[55] T. Luukkonen, "Modelling and Control of Quadcopter," *Independent research project, Espoo*, vol. 22, no. 22, pp. 1-24, 2011, https://sal.aalto.fi/publications/pdf-files/eluu11_public.pdf.

[56] S. Bouabdallah. *Design and Control of Quadrotors with Application to Autonomous Flying*. Doctoral dissertation, Epfl, 2007, https://infoscience.epfl.ch/entities/publication/4fbc8fc8-1a21-4a08-a24d-98f8302630f8.

[57] B. Bekhiti, K. Hariche, V. Zaitsev, G. R. Duan, and A. N. Sharkawy, "The Algebraic Theory of Operator Matrix Polynomials with Applications to Aeroelasticity in Flight Dynamics and Control," *Mathematical and Computational Applications*, vol. 30, no. 6, p. 131, 2025, https://doi.org/10.3390/mca30060131.

[58] S. F. Tolue and M. Moallem, "Multivariable sliding-mode extremum seeking control with application to alternator maximum power point tracking," *IECON 2016 - 42nd Annual Conference of the IEEE Industrial Electronics Society*, pp. 229-234, 2016, https://doi.org/10.1109/IECON.2016.7793319.

[59] L. Hu *et al*., "Sliding mode extremum seeking control based on improved invasive weed optimization for MPPT in wind energy conversion systems," *Applied Energy*, vol. 248, pp. 567–575, 2019, https://doi.org/10.1016/j.apenergy.2019.04.073.

[60] M. Krstic and H. H. Wang, "Stability of extremum seeking feedback for general nonlinear," *Automatica*, vol. 36, no. 4, pp. 595-601, 2000, https://doi.org/10.1016/S0005-1098(99)00183-1.